A time-domain method to solve transient elastic wave propagation in a multilayer medium with a hybrid spectral-finite element space approximation

Christophe Desceliers, Christian Soize, Q. Grimal, G. Haïat, S. Naili

A time domain method to solve transient elastic wave propagation in a multilayer medium with a hybrid spectral-finite element space approximation

C. Desceliers [a] C. Soize [a] Q. Grimal [b] G. Haiat [c] S. Naili [c]

[a] *Université Paris-Est, Laboratoire de Mécanique, 5 bd Descartes, 77454 Marne la Vallée Cedex 2, France*

[b] *Université Paris 6, Laboratoire d'Imagerie Paramétrique, France*

[c] *Université Paris 12, Laboratoire de Mécanique Physique, France*

Abstract

This paper introduces a new numerical hybrid method to simulate transient wave propagation in a multilayer semi-infinite medium, which can be fluid or solid, subjected to given transient loads. The medium is constituted of a finite number of unbounded layers with finite thicknesses. The method has a low numerical cost and is relatively straightforward to implement, as opposed to most available numerical techniques devoted to similar problems. The proposed method is based on a time-domain formulation associated with a 2D-space Fourier transform for the variables associated with the two infinite dimensions and uses a finite element approximation in the direction perpendicular to the layers. An illustration of the method is given for an elasto-acoustic wave propagation problem: a three-layer medium constituted of an elastic layer sandwiched between two acoustic fluid layers and excited by an acoustic line source located in one fluid layer.

Key words: Elastic and acoustic waves, finite element, multilayers, time-domain, low numerical cost

1 Introduction

The analysis of wave phenomena in layered elastic and acoustic media plays a fundamental role in the fields of non-destructive testing, geophysics and seismology. The textbooks devoted to the subject [1; 2; 7; 8; 22; 26] have reviewed

various formulations which take advantage of the problem symmetry to formulate algebraic problems for which analytical or semi-analytical solutions can be derived. The boundary value problem is usually solved either in the frequency-domain or in the time domain. Concerning the frequency-domain (Fourier transform with respect to time) two main strategies are generally used. The first one consists in a 3D-spectral (or 3D-wave-number) domain formulation (Fourier transform with respect to the space domain) [9; 27; 29; 38; 46] and the second one is a 2D-spectral (or 2D-wave-number) domain formulation (Fourier Transform with respect to the two infinite dimensions of the space domain) for which the boundary value problem is solved in a 1D-space domain (corresponding to the third finite dimension)[13; 39]. Such methods can induce numerical difficulties which can be avoided by using an adapted algebraic formulation which can be tricky to implement (see for instance [13]).

Concerning time-domain methods, two strategies are generally used. The first one consists in using numerical methods such as the finite volume time-domain method [5], the finite difference time-domain method [3; 14–16; 24; 28; 30; 32; 36; 40–43; 45] and the finite element method [4; 17–21; 47]. The second strategy consists in using analytical methods such as generalized-ray/Cagniard-de Hoop technique which is, as far as we know, the only available time-domain exact analytical method [8; 11; 12]. Although the theoretical time-domain formulations exist for complex situations (see for instance [12; 25; 31; 33; 34; 44]) such as 3D problem, anisotropic layers, property gradients, or attenuating media, analytical methods are hardly useful in practice, when several layers are involved, due tricky and configuration-specific implementations.

The purpose of this paper is to present a fast, hybrid numerical method to simulate the transient elastic wave propagation in multilayer semi-infinite media subjected to given transient loads. The proposed method is based on a time-domain formulation associated with a 2D-space Fourier transform for the two infinite layer dimensions and uses a finite element approximation in the direction perpendicular to the layers. This is an extension of semi-analytical methods [47] for which the symmetry of the problem is taken into account by

applying a spatial discrete Fourier transform for the directions for which the system is periodic. In this paper, the system is not periodic in any directions. Nevertheless, the mechanical and geometrical properties of the systems under consideration are assumed to be homogeneous for the two directions parallel to the layers. A spatial Fourier transform along these directions is then applied to the equations of boundary value problem. Generally, people also use a frequency formulation by applying a Fourier transform in time. Because the proposed method uses a time-domain formulation, the computational cost of the transient response of the system is expected to be low at relatively short times compared to the techniques based on Fourier transform in time. Note that the use of a Fourier transform to go in the frequency domain would require the calculation over a broad frequency band, thus increasing the numerical cost. Furthermore, the method is relatively straightforward to implement. The proposed method is an alternative to analytical techniques in complex situations but is limited to simple geometrical configuration (unbounded plane layers); for more complex geometries, finite elements or finite difference methods must be used.

The method can be used for 3D problems and arbitrary number of layers. However, in the present paper, for the purpose of illustration, the principle of the method is detailed for a particular 2D configuration in a layered medium consisting of a one elastic anisotropic layer sandwiched between two acoustic layers. An acoustic line source located in one of the two acoustic fluid layers generated the wave motion in the layered medium.

First, the 3D boundary value problem is written in 1D-space and 2D-spectral domains with a time-domain formulation (sections 2). Then, the equations are specified for the particular 2D problem used for illustration (sections 3). In section 3, the derivation of the space-spectral problem is given. In section 5, the weak formulation of the 1D-space, time-domain, boundary problem is introduced and the finite element approximation for the 1D-space is constructed (section 6). The implicit time integration scheme used for solving the differential equation in time is explained in section 7. The 2D-space solution in time is

then obtained by an inverse 1D-space Fourier transform. Section 8 is devoted to a numerical example which demonstrates the applicability of the method to investigate elasto-acoustics wave phenomena.

2 Three dimensional boundary value problem in the 3D-space with a time-domain formulation

We consider a three-dimensional multilayer medium composed of one elastic solid layer sandwiched between two acoustic fluid layers (see Figure 1). Let $\mathbf{R}(O, \mathbf{e}_1, \mathbf{e}_2, \mathbf{e}_3)$ be the reference Cartesian frame where O is the origin of the space and $(\mathbf{e}_1, \mathbf{e}_2, \mathbf{e}_3)$ is an orthonormal basis for this space. The coordinate of the generic point $\mathbf{x}$ in $\mathbb{R}$ is specified by (x_1, x_2, x_3). The thicknesses of the layers are denoted by h_1, h and h_2. The first acoustic fluid layer occupies the open unbounded domain Ω_1 , the second acoustic fluid layer occupies the open unbounded domain Ω_2 and the elastic solid layer occupies the open unbounded domain Ω. Let $\partial\Omega_1 = \Gamma_1 \cup \Gamma_0$, $\partial\Omega = \Gamma_0 \cup \Gamma$ and $\partial\Omega_2 = \Gamma \cup \Gamma_2$ (see Figure 1) be respectively the boundaries of Ω_1, Ω and Ω_2 in which $\Gamma_1, \Gamma_0, \Gamma$ and Γ_2 are the planes defined by

$$\Gamma_1 = \{x_1 \in \mathbb{R}\,, \quad x_2 \in \mathbb{R}\,, x_3 = z_1\}$$
$$\Gamma_0 = \{x_1 \in \mathbb{R}\,, \quad x_2 \in \mathbb{R}\,, x_3 = 0\}$$
$$\Gamma = \{x_1 \in \mathbb{R}\,, \quad x_2 \in \mathbb{R}\,, x_3 = z\}$$
$$\Gamma_2 = \{x_1 \in \mathbb{R}\,, \quad x_2 \in \mathbb{R}\,, x_3 = z_2\}$$

in which $z_1 = h_1$, $z = -h$ and $z_2 = -(h + h_2)$. Therefore, the domains Ω_1, Ω and Ω_2 are unbounded along the transversal directions $\mathbf{e}_1$ and $\mathbf{e}_2$ whereas they are bounded along the vertical direction $\mathbf{e}_3$.

The boundary conditions at the interfaces between solid and fluids are respectively defined by Eqs. (3) , (6) and (11) corresponding to the usual boundary conditions for acoustic fluids and linear elasticity for the solid (for instance, we refer the reader to [35; 37]).

The displacement field of a particle located in point $\mathbf{x}$ of Ω and at time $t > 0$ is

denoted by $\mathbf{u}(\mathbf{x},t) = (u_1(\mathbf{x},t), u_2(\mathbf{x},t), u_3(\mathbf{x},t))$. For all $\mathbf{x}$ belonging to Ω_1 and for all time $t > 0$, the disturbance of the pressure of the acoustic fluid layer occupying the domain Ω_1 is denoted by $p_1(\mathbf{x},t)$. The boundary value problem for this acoustic fluid layer is written as

$$\frac{1}{K_1}\frac{\partial^2 p_1}{\partial t^2} - \frac{1}{\rho_1}\Delta p_1 = \frac{1}{\rho_1}\frac{\partial Q}{\partial t} \quad , \ \mathbf{x} \in \Omega_1 \tag{1}$$

$$p_1 = 0 \quad , \ \mathbf{x} \in \Gamma_1 \tag{2}$$

$$\frac{\partial p_1}{\partial x_3} = -\rho_1 \frac{\partial^2 u_3}{\partial t^2} \quad , \ \mathbf{x} \in \Gamma_0 \tag{3}$$

in which $K_1 = \rho_1 c_1^2$ where c_1 and ρ_1 are, respectively,the wave velocity in the fluid and the mass density of the fluid at equilibrium; Δ is the Laplacian operator with respect to $\mathbf{x}$ and $Q(\mathbf{x},t)$ is the acoustic source density at point $\mathbf{x} = (x_1, x_2, x_3)$ and at time $t > 0$. This acoustic fluid is assumed to be subjected to an impulse line source located at positions (x_1^S, x_2^S, x_3^S) where x_1^S and x_3^S are given parameters fixed in $\mathbb{R}$ and where x_2^S runs in $\mathbb{R}$. The acoustic source density is assumed to be such that

$$\frac{\partial Q}{\partial t}(\mathbf{x},t) = \rho_1 F(t)\delta_0(x_1 - x_1^S)\delta_0(x_3 - x_3^S) \quad , \tag{4}$$

where $t \mapsto F(t)$ is a given function and δ_0 is the Dirac function in $\mathbb{R}$ at the origin.

The displacement field $\mathbf{u}$ of the solid elastic medium occupying the domain Ω verifies the following boundary value problem,

$$\rho\frac{\partial^2 \mathbf{u}}{\partial t^2} - \mathrm{div}\boldsymbol{\sigma} = \mathbf{0} \quad , \ \mathbf{x} \in \Omega \tag{5}$$

$$\boldsymbol{\sigma}\,\mathbf{n} = -p_1\,\mathbf{n} \quad , \ \mathbf{x} \in \Gamma_0 \tag{6}$$

$$\boldsymbol{\sigma}\,\mathbf{n} = -p_2\,\mathbf{n} \quad , \ \mathbf{x} \in \Gamma \tag{7}$$

in which ρ is the mass density and $\boldsymbol{\sigma}(\mathbf{x},t)$ is the Cauchy stress tensor of the solid elastic medium at point $\mathbf{x}$ and at time $t > 0$, $\mathbf{n}$ is the outward unit normal to domain Ω and div is the divergence operator with respect to $\mathbf{x}$. The constitutive equation of the solid elastic medium is written as

$$\boldsymbol{\sigma}(\mathbf{x},t) = \sum_{i,j,k,h=1}^{3} c_{ijkh}\varepsilon_{kh}(\mathbf{x},t)\,\mathbf{e}_i \otimes \mathbf{e}_j \tag{8}$$

in which $\sum_{i,j,k,h=1}^{3} c_{ijkh}\mathbf{e}_i \otimes \mathbf{e}_j \otimes \mathbf{e}_k \otimes \mathbf{e}_h$ is the elasticity tensor of the medium and $\varepsilon_{kh} = \frac{1}{2}(\frac{\partial u_k}{\partial x_h} + \frac{\partial u_h}{\partial x_k})$ is the linearized strain tensor.

For all $\mathbf{x}$ belonging to Ω_2 and for all time $t > 0$, the disturbance $p_2(\mathbf{x}, t)$ of the pressure of the acoustic fluid occupying the domain Ω_2 is such that

$$\frac{1}{K_2}\frac{\partial^2 p_2}{\partial t^2} - \frac{1}{\rho_2}\Delta p_2 = 0 \quad , \ \mathbf{x} \in \Omega_2 \tag{9}$$

$$p_2 = 0 \quad , \ \mathbf{x} \in \Gamma_2 \tag{10}$$

$$\frac{\partial p_2}{\partial x_3} = -\rho_2 \frac{\partial^2 u_3}{\partial t^2} \quad , \ \mathbf{x} \in \Gamma \tag{11}$$

in which $K_2 = \rho_2\, c_2^2$ where c_2 and ρ_2 are, respectively, the wave velocity in the fluid and the mass density of the fluid at equilibrium.

Furthermore, the system is at rest at time $t = 0$. Consequently, we have

$$p_1(\mathbf{x}, 0) = 0 \quad , \ \mathbf{x} \in \Omega_1 \cup \partial\Omega_1 \tag{12}$$

$$\mathbf{u}(\mathbf{x}, 0) = 0 \quad , \ \mathbf{x} \in \Omega \cup \partial\Omega \tag{13}$$

$$p_2(\mathbf{x}, 0) = 0 \quad , \ \mathbf{x} \in \Omega_2 \cup \partial\Omega_2 \tag{14}$$

3 Two dimensional boundary value problems in the 2D-space with a time-domain formulation

At $t = 0$, a line source parallel to $(O; \mathbf{x}_2)$, placed in the fluid Ω_1 at a given distance from the interface Γ_0 generates a cylindrical wave. Due to the nature of the source and to the geometrical configuration, the transverse waves polarized in the $(\mathbf{e}_1, \mathbf{e}_2)$ plane are not excited. The present study is conducted in the plane $(O; \mathbf{e}_1, \mathbf{e}_3)$. The total elasto-acoustic wave motion will be independent of x_2, hence all derivatives with respect to x_2 vanish in the partial differential equations that govern the wave motion. Consequently, coordinate x_2 is implicit in the mathematical expressions to follow. In the following, in order to simplify the notation, $\mathbf{u}$ is rewritten as $\mathbf{u}(x_1, x_3, t) = (u_1(x_1, x_3, t), u_3(x_1, x_3, t))$. Taking into account this symmetry, the 3D-boundary value problem yields the following 2D-boundary value problem in the 2D-space domain which is

written as

$$\frac{1}{K_1}\frac{\partial^2 p_1}{\partial t^2} - \frac{1}{\rho_1}\frac{\partial^2 p_1}{\partial x_1^2} - \frac{1}{\rho_1}\frac{\partial^2 p_1}{\partial x_3^2} = \frac{1}{\rho_1}\frac{\partial Q}{\partial t} \quad , \ \mathbf{x} \in \Omega_1 \tag{15}$$

$$p_1 = 0 \quad , \ \mathbf{x} \in \Gamma_1 \tag{16}$$

$$\frac{\partial p_1}{\partial x_3} = -\rho_1 \frac{\partial^2 u_3}{\partial t^2} \quad , \ \mathbf{x} \in \Gamma_0 \tag{17}$$

$$\rho\frac{\partial^2 u_1}{\partial t^2} - \frac{\partial \sigma_{11}}{\partial x_1} - \frac{\partial \sigma_{13}}{\partial x_3} = 0 \quad , \quad \rho\frac{\partial^2 u_3}{\partial t^2} - \frac{\partial \sigma_{13}}{\partial x_1} - \frac{\partial \sigma_{33}}{\partial x_3} = 0 \quad , \ \mathbf{x} \in \Omega \tag{18}$$

$$\sigma_{13} = 0 \quad , \quad \sigma_{33} = -p_1 \quad , \ \mathbf{x} \in \Gamma_0 \tag{19}$$

$$\sigma_{13} = 0 \quad , \quad \sigma_{33} = -p_2 \quad , \ \mathbf{x} \in \Gamma \tag{20}$$

$$\frac{1}{K_2}\frac{\partial^2 p_2}{\partial t^2} - \frac{1}{\rho_2}\frac{\partial^2 p_2}{\partial x_1^2} - \frac{1}{\rho_2}\frac{\partial^2 p_2}{\partial x_3^2} = 0 \quad , \ \mathbf{x} \in \Omega_2 \tag{21}$$

$$p_2 = 0 \quad , \ \mathbf{x} \in \Gamma_2 \tag{22}$$

$$\frac{\partial p_2}{\partial x_3} = -\rho_2 \frac{\partial^2 u_3}{\partial t^2} \quad , \ \mathbf{x} \in \Gamma \tag{23}$$

where

$$\sigma_{11} = \widetilde{c}_{11}\frac{\partial u_1}{\partial x_1} + \widetilde{c}_{12}\frac{\partial u_3}{\partial x_3} + \frac{\sqrt{2}}{2}\widetilde{c}_{13}\left(\frac{\partial u_3}{\partial x_1} + \frac{\partial u_1}{\partial x_3}\right) \tag{24}$$

$$\sigma_{13} = \frac{\sqrt{2}}{2}\widetilde{c}_{31}\frac{\partial u_1}{\partial x_1} + \frac{\sqrt{2}}{2}\widetilde{c}_{32}\frac{\partial u_3}{\partial x_3} + \frac{1}{2}\widetilde{c}_{33}\left(\frac{\partial u_3}{\partial x_1} + \frac{\partial u_1}{\partial x_3}\right) \tag{25}$$

$$\sigma_{33} = \widetilde{c}_{21}\frac{\partial u_1}{\partial x_1} + \widetilde{c}_{22}\frac{\partial u_3}{\partial x_3} + \frac{\sqrt{2}}{2}\widetilde{c}_{23}\left(\frac{\partial u_3}{\partial x_1} + \frac{\partial u_1}{\partial x_3}\right) \tag{26}$$

in which, for $\{i,j\} \subset \{1,2,3\}$, $\widetilde{c}_{ij}$ are the components of the matrix $[\widetilde{C}]$ defined as

$$[\widetilde{C}] = \begin{bmatrix} c_{1111} & c_{1133} & \sqrt{2}c_{1131} \\ c_{3311} & c_{3333} & \sqrt{2}c_{3331} \\ \sqrt{2}c_{3111} & \sqrt{2}c_{3133} & 2c_{3131} \end{bmatrix}$$

4 One dimensional boundary value problem in the 1D-spectral domain with a time-domain formulation

For all x_3 fixed in $]z_2, z_1[$, the 1D-Fourier transform of an integrable function $x_1 \mapsto f(x_1, x_3, t)$ on $\mathbb{R}$ is defined by

$$\widehat{f}(k_1, x_3, t) = \int_{\mathbb{R}} f(x_1, x_3, t)\, e^{i\,k_1\,x_1} dx_1 \quad .$$

Applying the 1D-Fourier transform to Eqs. (1) to (13) yields the 1D boundary value problem of the system in the 1D space domain with a 1D-spectral and time domains formulation. Such a boundary value problem is written with respect to the functions $\widehat{p}_1$, $\widehat{\mathbf{u}}$ and $\widehat{p}_2$ which are respectively the 1D-Fourier transforms of functions p_1, $\mathbf{u}$ and p_2. We then have

$$\frac{1}{K_1}\frac{\partial^2 \widehat{p}_1}{\partial t^2} + \frac{k_1^2}{\rho_1}\widehat{p}_1 - \frac{1}{\rho_1}\frac{\partial^2 \widehat{p}_1}{\partial x_3^2} = F(t)\,\mathrm{e}^{ik_1 x_1^S}\,\delta_0(x_3 - x_3^S) \quad \text{for} \quad x_3 \in]0, z_1[$$
$$\widehat{p}_1 = 0 \quad \text{for} \quad x_3 = z_1$$
$$\frac{\partial \widehat{p}_1}{\partial x_3} = -\rho_1 \frac{\partial^2 \widehat{u}_3}{\partial t^2} \quad \text{for} \quad x_3 = 0$$
$$\rho\frac{\partial^2 \widehat{u}_1}{\partial t^2} + ik_1\widehat{\sigma}_{11} - \frac{\partial \widehat{\sigma}_{13}}{\partial x_3} = 0 \quad , \quad \rho\frac{\partial^2 \widehat{u}_3}{\partial t^2} + ik_1\widehat{\sigma}_{13} - \frac{\partial \widehat{\sigma}_{33}}{\partial x_1} = 0 \quad \text{for} \quad x_3 \in]z, 0[$$
$$\widehat{\sigma}_{13} = 0 \quad \text{and} \quad \widehat{\sigma}_{33} = -\widehat{p}_1 \quad \text{for} \quad x_3 = 0$$
$$\widehat{\sigma}_{13} = 0 \quad \text{and} \quad \widehat{\sigma}_{33} = -\widehat{p}_2 \quad \text{for} \quad x_3 = z$$
$$\frac{1}{K_2}\frac{\partial^2 \widehat{p}_2}{\partial t^2} + \frac{k_1^2}{\rho_2}\widehat{p}_2 - \frac{1}{\rho_2}\frac{\partial^2 \widehat{p}_2}{\partial x_3^2} = 0 \quad \text{for} \quad x_3 \in]z_2, z[$$
$$\widehat{p}_2 = 0 \quad \text{for} \quad x_3 = z_2$$
$$\frac{\partial \widehat{p}_2}{\partial x_3} = -\rho_2 \frac{\partial^2 \widehat{u}_3}{\partial t^2} \quad \text{for} \quad x_3 = z$$

in which

$$\widehat{\sigma}_{11} = -ik_1\widetilde{c}_{11}\widehat{u}_1 + \widetilde{c}_{12}\frac{\partial \widehat{u}_3}{\partial x_3} - ik_1\frac{\sqrt{2}}{2}\widetilde{c}_{13}\widehat{u}_3 + \frac{\sqrt{2}}{2}\widetilde{c}_{13}\frac{\partial \widehat{u}_1}{\partial x_3}$$
$$\widehat{\sigma}_{13} = -ik_1\frac{\sqrt{2}}{2}\widetilde{c}_{31}\widehat{u}_1 + \frac{\sqrt{2}}{2}\widetilde{c}_{32}\frac{\partial \widehat{u}_3}{\partial x_3} - ik_1\frac{\widetilde{c}_{33}}{2}\widehat{u}_3 + \frac{\widetilde{c}_{33}}{2}\frac{\partial \widehat{u}_1}{\partial x_3}$$
$$\widehat{\sigma}_{33} = -ik_1\widetilde{c}_{21}\widehat{u}_1 + \widetilde{c}_{22}\frac{\partial \widehat{u}_3}{\partial x_3} - ik_1\frac{\sqrt{2}}{2}\widetilde{c}_{23}\widehat{u}_3 + \frac{\sqrt{2}}{2}\widetilde{c}_{23}\frac{\partial \widehat{u}_1}{\partial x_3}$$

5 Weak formulation in the 1D-spectral domain with a time-domain formulation

Let $\mathscr{C}_1$ and $\mathscr{C}_2$ be the function spaces constituted of all the sufficiently differentiable complex-valued functions $x_3 \mapsto \delta p_1(x_3)$ and $x_3 \mapsto \delta p_2(x_3)$ respectively, defined on $]0, z_1[$ and $]z_2, z[$. We introduce the admissible function spaces $\mathscr{C}_{1,0} \subset \mathscr{C}_1$ and $\mathscr{C}_{2,0} \subset \mathscr{C}_2$ such that

$$\mathscr{C}_{1,0} = \{\delta p_1 \in \mathscr{C}_1; \quad \delta p_1(z_1) = 0\}$$

$$\mathscr{C}_{2,0} = \{\delta p_2 \in \mathscr{C}_2; \quad \delta p_2(z_2) = 0\}$$

Let $\mathscr{C}$ be the admissible function space constituted of all the sufficiently differentiable functions $x_3 \mapsto \delta\mathbf{u}(x_3)$ from $]z, 0[$ into $\mathbb{C}^2$ where $\mathbb{C}$ is the set of all the complex numbers.

The weak formulation of the 1D boundary value problem is written as : for all k_1 fixed in $\mathbb{R}$ and for all fixed t, find $\widehat{p}_1(k_1, \cdot, t) \in \mathscr{C}_{1,0}$, $\widehat{\mathbf{u}}(k_1, \cdot, t) \in \mathscr{C}$ and $\widehat{p}_2(k_1, \cdot, t) \in \mathscr{C}_{2,0}$ such that, for all $\delta p_1 \in \mathscr{C}_{1,0}$, $\delta\mathbf{u} \in \mathscr{C}$ and $\delta p_2 \in \mathscr{C}_{2,0}$,

$$\begin{aligned}
&a_1\left(\frac{\partial^2\widehat{p}_1}{\partial t^2}, \delta p_1\right) + k_1^2\, c_1^2\, a_1(\widehat{p}_1, \delta p_1) + b_1(\widehat{p}_1, \delta p_1) + r_1\left(\frac{\partial^2\widehat{\mathbf{u}}}{\partial t^2}, \delta p_1\right) = f(\delta p_1; t)\ , \\
&m\left(\frac{\partial^2\widehat{\mathbf{u}}}{\partial t^2}, \delta\mathbf{u}\right) + s_1(\widehat{\mathbf{u}}, \delta\mathbf{u}) + k_1^2\, s_2(\widehat{\mathbf{u}}, \delta\mathbf{u}) - ik_1\, s_3(\widehat{\mathbf{u}}, \delta\mathbf{u}) + \overline{r_2(\delta\mathbf{u}, \widehat{p}_2)} - \overline{r_1(\delta\mathbf{u}, \widehat{p}_1)} = 0\ , \\
&a_2\left(\frac{\partial^2\widehat{p}_2}{\partial t^2}, \delta p_2\right) + k_1^2\, c_2^2\, a_2(\widehat{p}_2, \delta p_2) + b_2(\widehat{p}_2, \delta p_2) - r_2\left(\frac{\partial^2\widehat{\mathbf{u}}}{\partial t^2}, \delta p_2\right) = 0\ ,
\end{aligned}$$

in which the sesquilinear forms and linear forms are given in Appendix A. In the above equations, the over-line denotes the complex conjugate, a_1 and b_1 are, respectively, positive-definite and positive sesquilinear forms on $\mathscr{C}_1 \times \mathscr{C}_1$, the sesquilinear form r_1 is defined on $\mathscr{C} \times \mathscr{C}_1$, the antilinear form f is defined on $\mathscr{C}_1$, the sesquilinear forms a_2 and b_2 are, respectively, positive-definite and positive on $\mathscr{C}_2 \times \mathscr{C}_2$, the sesquilinear form r_2 is defined on $\mathscr{C} \times \mathscr{C}_2$, the sesquilinear forms m and s_2 are, respectively, positive-definite on $\mathscr{C} \times \mathscr{C}$, the sesquilinear form s_1 is positive on $\mathscr{C} \times \mathscr{C}$ and finally, the sesquilinear form s_3 is skew-symmetric on $\mathscr{C} \times \mathscr{C}$.

6 Finite element approximation

We introduce a finite element mesh of domain $[z_2, z] \cup [z, 0] \cup [0, z_1]$ which is constituted of ν_{tot} nodes. The finite elements used are Lagrangian 1D-finite element with 3 nodes. Let $\widehat{\mathbf{p}}_1(k_1, t)$, $\widehat{\mathbf{v}}(k_1, t)$ and $\widehat{\mathbf{p}}_2(k_1, t)$ be the complex vectors of the nodal values of the functions $x_3 \mapsto \widehat{p}_1(k_1, x_3, t)$, $x_3 \mapsto \widehat{\mathbf{u}}(k_1, x_3, t)$ and $x_3 \mapsto \widehat{p}_2(k_1, x_3, t)$. Let $\widehat{\mathbf{f}}(k_1, t)$ be the complex vector in $\mathbb{C}^{\nu_1}$ where ν_1 is the number of degree of freedom related to the mesh of domain $[0, z_1]$, corre-

sponding to the finite element approximation of the antilinear form $f(\delta p_1; t)$. For all k_1 fixed in $\mathbb{R}$ and for all fixed t, the finite element approximation of the weak formulation of the 1D boundary value problem yields the following linear system of equations

$$[A_1]\,\ddot{\widehat{\mathbf{p}}}_1 + (k_1^2\,c_1^2[A_1]\ + [B_1])\widehat{\mathbf{p}}_1(k_1,t) + [R_1]\,\ddot{\widehat{\mathbf{v}}}(k_1,t) = \widehat{\mathbf{f}}(k_1,t) \tag{27}$$

$$[M]\,\ddot{\widehat{\mathbf{v}}}(k_1,t) + ([S_1] - ik_1\,[S_3] + k_1^2\,[S_2])\widehat{\mathbf{v}}(k_1,t) + [R_2]^T\,\widehat{\mathbf{p}}_2(k_1,t) - [R_1]^T\,\widehat{\mathbf{p}}_1(k_1,t) = 0 \tag{28}$$

$$[A_2]\,\ddot{\widehat{\mathbf{p}}}_2(k_1,t) + (k_1^2\,c_2^2[A_2] + [B_2])\widehat{\mathbf{p}}_2(k_1,t) - [R_2]\,\ddot{\widehat{\mathbf{v}}}(k_1,t) = 0 \tag{29}$$

in which the double dots means the second partial derivative with respect to t. Each of Eqs. (27) , (28) and (29) form linear systems whose the square matrices are respectively of dimensions $\nu_1 \times \nu_1$, $\nu \times \nu$ and $\nu_2 \times \nu_2$. The integer numbers ν and ν_2 are respectively the number of degree of freedom related to the meshes of domains $[z, 0]$ and $[z_2, z]$. Moreover, the components of these matrices are complex numbers. These three equations can be rewritten as

$$[\mathbb{M}]\,\ddot{\widehat{\mathbb{v}}}(k_1,t) + ([\mathbb{K}_1] - ik_1[\mathbb{K}_2] + k_1^2[\mathbb{K}_3])\widehat{\mathbb{v}}(k_1,t) = \widehat{\mathbb{f}}(k_1,t) \tag{30}$$

in which the vectors $\widehat{\mathbb{v}}(k_1,t) = (\widehat{\mathbf{p}}_1(k_1,t), \widehat{\mathbf{v}}(k_1,t), \widehat{\mathbf{p}}_2(k_1,t))$ and $\widehat{\mathbb{f}}(k_1,t) = (\widehat{\mathbf{f}}(k_1,t), 0, 0)$ belong to $\mathbb{C}^{\nu_1+\nu+\nu_2}$ and where

$$[\mathbb{M}] = \begin{bmatrix} [A_1] & [R_1] & 0 \\ 0 & [M] & 0 \\ 0 & -[R_2] & [A_2] \end{bmatrix}, \qquad [\mathbb{K}_1] = \begin{bmatrix} [B_1] & 0 & 0 \\ -[R_1]^T & [S_1] & [R_2]^T \\ 0 & 0 & [B_2] \end{bmatrix}$$

$$[\mathbb{K}_2] = \begin{bmatrix} 0 & 0 & 0 \\ 0 & [S_3] & 0 \\ 0 & 0 & 0 \end{bmatrix}, \qquad [\mathbb{K}_3] = \begin{bmatrix} c_1^2\,[A_1] & 0 & 0 \\ 0 & [S_2] & 0 \\ 0 & 0 & c_2^2\,[A_2] \end{bmatrix}$$

where $\cdot^T$ designates the transpose operator.

7 Numerical solver

7.1 Time and space sampling

The solution $t \mapsto \widehat{\mathbb{v}}(k_1,t)$ of Eq. (30) is constructed for all k_1 belonging to a broad spectral band of analysis $[-k_{1,max}, k_{1,max}]$ and for t belong-

ing to a time domain of analysis $[0, T_{max}]$. Let Δk_1 and let Δt be spectral (wave number) and time sampling steps such that $k_{1,max} = M\Delta k_1/2$ and $T_{\max} = N\Delta t$ where M is an odd integer and N is any integer. Shannon's theorem yields $\Delta x_1 = 2\pi/(2k_{1,max}) = 2\pi/(M\Delta k_1)$ and $\Delta t = 1/(2\, f_{max})$ where $[-f_{max}, f_{max}]$ is the frequency band of analysis. Consequently, x_1 belongs to the space domain $[-x_{1,max}, x_{1,max}]$ with $x_{1,max} = M\Delta x_1/2 = \pi/\Delta k_1$. Let $\widehat{\mathbb{v}}^{n,m} = (\widehat{\mathbf{p}}_1^{n,m}, \widehat{\mathbf{v}}^{n,m}, \widehat{\mathbf{p}}_2^{n,m})$ be the solution of Eq. (30) at time t_n and for wave-number $k_{1,m}$ which are such that, for all $n = 0, \ldots, N$ and $m = 0, \ldots, M-1$

$$t_n = n\Delta t \quad \text{and} \quad k_{1,m} = m\,\Delta k_1 - k_{1,max} \quad ,$$

For all $n = 0, \ldots, N$ and $m = 0, \ldots, M-1$, we introduce the vectors $\dot{\widehat{\mathbb{v}}}^{n,m} = (\dot{\widehat{\mathbf{p}}}_1^{n,m}, \dot{\widehat{\mathbf{v}}}^{n,m}, \dot{\widehat{\mathbf{p}}}_2^{n,m})$ and $\ddot{\widehat{\mathbb{v}}}^{n,m} = (\ddot{\widehat{\mathbf{p}}}_1^{n,m}, \ddot{\widehat{\mathbf{v}}}^{n,m}, \ddot{\widehat{\mathbf{p}}}_2^{n,m})$ respectively defined as the first and the second partial derivatives of $t \mapsto \mathbb{v}(k_{1,m}, t)$ at time t_n. We then have

$$\widehat{\mathbb{v}}^{n,m} = \widehat{\mathbb{v}}(k_{1,m},\ t_n) \quad . \tag{31}$$

$$\dot{\widehat{\mathbb{v}}}^{n,m} = \dot{\widehat{\mathbb{v}}}(k_{1,m},\ t_n) \quad , \tag{32}$$

$$\ddot{\widehat{\mathbb{v}}}^{n,m} = \ddot{\widehat{\mathbb{v}}}(k_{1,m},\ t_n) \quad . \tag{33}$$

For $t = t_{n+1}$ and $k_1 = k_{1,m}$, Eq. (30) is rewritten as

$$[\mathbb{M}]\,\ddot{\widehat{\mathbb{v}}}^{n+1,m} + ([\mathbb{K}_1] - ik_{1,m}([\mathbb{K}_2] + k_{1,m}^2[\mathbb{K}_3])\widehat{\mathbb{v}}^{n+1,m} = \widehat{\mathbb{f}}^{n+1,m} \quad , \tag{34}$$

in which $\widehat{\mathbb{f}}^{n+1,m} = \widehat{\mathbb{f}}(k_{1,m},\ t_{n+1})$.

7.2 Time domain solver for fixed wave-number

An implicit unconditionally stable Newmark scheme (see [4; 47]) is used to solve Eq. (30) in time. Consequently, for all $n = 0, \ldots, N-1$ and $m = 0, \ldots, M-1$, we have

$$\dot{\widehat{\mathbb{v}}}^{n+1,m} = \dot{\widehat{\mathbb{v}}}^{n,m} + \left[(1-\delta)\ddot{\widehat{\mathbb{v}}}^{n,m} + \delta\,\ddot{\widehat{\mathbb{v}}}^{n+1,m}\right]\Delta t \quad , \tag{35}$$

$$\widehat{\mathbb{v}}^{n+1,m} = \widehat{\mathbb{v}}^{n,m} + \dot{\widehat{\mathbb{v}}}^{n,m}\,\Delta t + \left[(0.5-\alpha)\,\ddot{\widehat{\mathbb{v}}}^{n,m} + \alpha\,\ddot{\widehat{\mathbb{v}}}^{n+1,m}\right]\Delta t^2 \quad , \tag{36}$$

where $\delta \geq 0.5$ and $\alpha \geq 0.25(0.5+\delta)^2$. Using Eqs. (34) to (36) yields

$$\Big([\mathbb{K}_1] - ik_{1,m}([\mathbb{K}_2] + k_{1,m}^2[\mathbb{K}_3] + a_0\ [\mathbb{M}]\Big)\,\widehat{\mathbb{v}}^{n+1,m} = \widetilde{\mathbb{g}}^{n+1,m} \quad , \tag{37}$$

in which

$$\widetilde{\mathbb{g}}^{n+1,m} = \widehat{\mathbb{f}}^{n+1,m} + [\mathbb{M}]\ \Big(a_0\,\widehat{\mathbb{v}}^{n,m} + a_1\,\dot{\widehat{\mathbb{v}}}^{n,m} + a_2\ddot{\widehat{\mathbb{v}}}^{n,m}\Big) \quad ,$$

and where $a_0 = 1/(\alpha\,\Delta t^2)$, $a_1 = 1/(\alpha\Delta t)$ and $a_2 = (0.5/\alpha) - 1$. The dynamical system being at rest at time $t = 0$, then, for all m, $\widehat{\mathbb{v}}^{0,m}$, $\dot{\widehat{\mathbb{v}}}^{0,m}$ and $\dot{\widehat{\mathbb{v}}}^{0,m}$ are equal to zero. Then, solving Eq. (37) , vectors $\widehat{\mathbb{v}}^{1,m}, \ldots, \widehat{\mathbb{v}}^{N,m}$ are calculated for all $m = 0, \ldots, M-1$

7.3 Space solver for fixed time

Let $\mathbb{v}(x_1,t) = (\mathbf{p}_1(x_1,t), \mathbf{v}(x_1,t), \mathbf{p}_2(x_1,t))$ be the vector of the nodal values of $x_3 \mapsto p_1(x_1,x_3,t)$, $x_3 \mapsto \mathbf{u}(x_1,x_3,t)$ and $x_3 \mapsto p_2(x_1,x_3,t)$ related to the finite element mesh of the domain $]z_2, z_1[$. We then have

$$\mathbb{v}(x_1,t) = \frac{1}{2\pi}\int_{\mathbb{R}} \widehat{\mathbb{v}}(k_1,t) e^{-i\,k_1\,x_1} dk_1 \quad . \tag{38}$$

For $n = 0, \ldots, N$ and $\ell = 0, \ldots, M-1$, let $\mathbb{v}^{n,\ell} = (\mathbf{p}_1^{n,\ell}, \mathbf{v}^{n,\ell}, \mathbf{p}_2^{n,\ell})$ be the vector equal to $\mathbb{v}(x_1,t)$ with $t = t_n$, $x_1 = x_{1,\ell}$ where $x_{1,\ell} = \ell\Delta x_1 - x_{1,max}$. We then have

$$\mathbb{v}^{n,\ell} = \mathbb{v}(x_{1,\ell},\ t_n) \quad . \tag{39}$$

For all $n = 0, \ldots, N$ and for all $\ell = 0, \ldots, M-1$, it can be shown that

$$\mathbb{v}^{n,\ell} = \frac{\Delta k_1}{2\pi}\, e^{i\pi(\ell - \frac{M}{2})}\, \mathbb{w}^{n,\ell} \quad , \tag{40}$$

where

$$\mathbb{w}^{n,\ell} = \sum_{m=0}^{M-1} \widehat{\mathbb{w}}^{n,m}\, e^{-\frac{2i\pi m\,\ell}{M}} \quad , \tag{41}$$

in which $\widehat{\mathbb{w}}^{n,m} = \widehat{\mathbb{v}}^{n,m}\, e^{i\,m\,\pi}$. The summation in Eq. (41) is performed using Fast Fourier Transform.

8 NUMERICAL EXAMPLES

8.1 Multilayer system with a solid transverse isotropic medium example

The configuration used for the numerical example presented here is an idealized model of the 'axial transmission' technique used to evaluate the mechanical properties of cortical bone [6; 31]. In this context, the solid and the fluid represent bone and soft tissues (skin, muscle, marrow), respectively.

The acoustic fluid layer Ω_1 is excited by a line source located at $x_1 = x_1^S$ and $x_3 = x_3^S$ (see Table 1) with a time-history defined with the function F in Eq. (4) such that

$$F(t) = F_1 \sin(2\pi f_c t) e^{-4(t\, f_c - 1)^2} \quad ,$$

where f_c is the center frequency and F_1 is a given parameter. Figure 2 shows the power spectrum of F (left) and the graph of function $t \mapsto F(t)$ (right).

h_1	10^{-2}m	h	4×10^{-3}m	h_2	10^{-2}m
ρ_1	1000 kg.m^{-3}	ρ	1722 kg.m^{-3}	ρ_2	1000 kg.m^{-3}
c_1	1500 m.s^{-1}	E_L	16.6 GPa	c_2	1500 m.s^{-1}
f_c	1 MHz	E_T	9.5 GPa		
x_1^S	0	ν_L	0.38		
x_3^S	2×10^{-3}m	ν_T	0.44		
F_1	100 m.s^{-2}	G_L	4.7 GPa		
		G_T	3.3 GPa		

Table 1. Values of the parameters. Material parameters stand for compact bone [31]

The elastic layer which occupies domain Ω is constituted of a transverse isotropic medium for which the plane (x_1, x_2) is the plane of isotropy. Such a material is completely defined with five independent elastic constants. We will use the longitudinal and transversal Young moduli denoted by E_L and E_T, respectively; the longitudinal and transversal shear moduli denoted by G_L and G_T, respectively; the longitudinal and transversal Poisson coefficients

denoted by ν_L and ν_T, respectively, where the relation

$$G_T = \frac{E_T}{2(1+\nu_T)} \quad .$$

holds between the coefficients. The numerical values of these mechanical parameters are given in Table 1. The coefficients $\widetilde{c}_{ij}$ of the matrix $[\widetilde{C}]$ are defined according to $\widetilde{c}_{23} = \widetilde{c}_{32} = \widetilde{c}_{31} = \widetilde{c}_{13} = 0$, $\widetilde{c}_{33} = 2\,G_L$, and

$$\widetilde{c}_{11} = \frac{E_L^2(1-\nu_T)}{(E_L - E_L\nu_T - 2E_T\nu_L^2)}, \quad \widetilde{c}_{22} = \frac{E_T(E_L - E_T\nu_L^2)}{(1+\nu_T)(E_L - E_L\nu_T - 2E_T\nu_L^2)},$$
$$\widetilde{c}_{12} = \widetilde{c}_{21} = \frac{E_T E_L \nu_L}{(E_L - E_L\nu_T - 2E_T\nu_L^2)} \quad .$$

The parameters used for the numerical method (time-domain approximation, spectral and finite element approximation) are given in Table 2.

T_{max}	N	ν_1	ν	ν_2	M	$x_{1,max}$	δ	α
2.5×10^{-5}	850	101	82	101	1024	0.2	0.5	0.25

Table 2. Parameters for the numerical method

8.1.1 Convergence analysis

In order to perform a convergence analysis of the proposed method with respect to the parameters N and M, we introduce the function $(N, M) \mapsto \mathrm{conv}(N, M; x_1, x_3)$ defined by

$$\mathrm{conv}(N, M; x_1, x_3) = \left(\sum_{n=0}^{N-1} |\mathbf{p}_{1,\nu}^{n,\ell}(N, M)|^2 \, \Delta t \right)^{\frac{1}{2}} \quad ,$$

where $\mathbf{p}_{1,\nu}^{n,\ell}(N, M)$ is the νth components of vector $\mathbf{p}_1^{n,\ell}$ which is the vector of the nodal values of $x_3 \mapsto p_1(\ell\,\Delta x_1 - x_{1,max}, x_3,\ n\Delta t)$ and which depends on parameters N and M. Figure 3 shows the graphs of function $N \mapsto \mathrm{conv}(N, M; x_1, x_3)$ with $M = 8192$ and $x_3 = 2 \times 10^{-3}$ m and for $x_1 = 8 \times 10^{-3}$ m (thick solid line), $x_1 = 12 \times 10^{-3}$ m (thin solid line), $x_1 = 20 \times 10^{-3}$ m (thick dashed line) and $x_1 = 28 \times 10^{-3}$ m. Figure 4 shows the graphs of function $M \mapsto \mathrm{conv}(N, M; x_1, x_3)$ with $N = 5000$ and $x_3 = 2 \times 10^{-3}$ m and for $x_1 = 8 \times 10^{-3}$ m (thick solid line), $x_1 = 12 \times 10^{-3}$ m (thin solid line),

$x_1 = 20 \times 10^{-3}$ m (thick dashed line) and $x_1 = 28 \times 10^{-3}$ m (thin dashed line). From these graphs, it can be deduced that, for this numerical example and for the observations point located at $x_1 = 8 \times 10^{-3}$ m , $x_1 = 12 \times 10^{-3}$ m , $x_1 = 20 \times 10^{-3}$ m and $x_1 = 28 \times 10^{-3}$ m with $x_3 = 2 \times 10^{-3}$ m, that convergence is reached for $N = 850$ and $M = 1024$.

8.1.2 Results

Let $\mathrm{vm}(\mathbf{x}, t)$ be the von Mises stress at point $\mathbf{x} \in \Omega$ and at time t. Figures 5(A) to (H) show the graphs of functions $(x_1, x_3) \mapsto p_1(x_1, x_3, t)$, $(x_1, x_3) \mapsto \mathrm{vm}(x_1, x_3, t)$ and $(x_1, x_3) \mapsto p_2(x_1, x_3, t)$ at $t = 1.56\,\mu$s (Fig. 5(A)), $t = 2.06\,\mu$s (Fig. 5(B)), $t = 2.94\,\mu$s (Fig. 5(C)), $t = 5.89\,\mu$s (Fig. 5(D)), $t = 9.72\,\mu$s (Fig. 5(E)), $t = 13.55\,\mu$s (Fig. 5(F)), $t = 15.31\,\mu$s (Fig. 5(G)), $t = 119.88\,\mu$s (Fig. 5(H)). It has to be noted that all the elastic waves propagation phenomena (close-field effects, refracted surface waves, reflection and transmission, etc) are simulated using this method since no kinematic simplifications are introduced. In particular, the material configuration considered is such that a lateral wave (or head wave) [7] propagates from the fluid-solid interface (plane wave front which links the reflected P-wave front and the interface); the lateral wave is a typical time-domain phenomena and is very well described by the method.

Finally, figure 6 shows the graphs of function $t \mapsto p_1(x_1, x_3, t)$ with $x_3 = 2 \times 10^{-3}$ m and for $x_1 = 8 \times 10^{-3}$ m (fig. 6(A)), $x_1 = 12 \times 10^{-3}$ m (fig. 6(B)), $x_1 = 20 \times 10^{-3}$ m (fig. 6(C)) and $x_1 = 28 \times 10^{-3}$ m (fig. 6(D)). The first perturbation arriving at the receivers is the contribution of the lateral wave; the largest amplitude contribution is the direct wave and the other contributions are the waves reflected in the multilayer system. From this point of view, these signals are consistent with the results presented in [31] obtained with an exact analytical method but in which a two layers fluid-solid system with infinite thicknesses was considered.

For this simulation, the total CPU time is 309 s and using a 3.8 MHz Xeon processor. The total amount of read access memory (RAM) used is 20 Mo. Such a CPU time and such a read access memory represent a very low computational

cost with respect to a method which would be based on a full finite element computation and for which more than 16 Go of RAM and more than 25000 s of CPU time is needed without reaching the same quality of approximation.

8.2 Multilayer system with a solid anisotropic medium example

For this example, we consider the same problem as in the previous section but the medium is assumed to be made of an anisotropic material for which the elasticity matrix is such that

$$[\widetilde{C}] = 10^{10} \times \begin{bmatrix} 0.7513 & -0.1054 & -0.2684 \\ -0.1054 & 0.5857 & 0.3941 \\ -0.2684 & 0.3941 & 1.3762 \end{bmatrix} \quad .$$

8.2.1 Results

Figures 7(A) to (H) show the graphs of functions $(x_1, x_3) \mapsto p_1(x_1, x_3, t)$, $(x_1, x_3) \mapsto \mathrm{vm}(x_1, x_3, t)$ and $(x_1, x_3) \mapsto p_2(x_1, x_3, t)$ at $t = 1.56\,\mu$s (Fig. 7(A)), $t = 2.06\,\mu$s (Fig. 7(B)), $t = 2.94\,\mu$s (Fig. 7(C)), $t = 5.89\,\mu$s (Fig. 7(D)), $t = 9.72\,\mu$s (Fig. 7(E)), $t = 13.55\,\mu$s (Fig. 7(F)), $t = 15.31\,\mu$s (Fig. 7(G)), $t = 119.88\,\mu$s (Fig. 7(H)). It has to be noted that, due to the anisotropy of the solid medium, the elastic waves propagation is not symmetric in the solid and the second fluid layers whereas the wave propagation in the first fluid layer is still symmetric. This can easily be explain by considering that the coupling between the first fluid layer and the solid layer is written as partial derivative equation on pressure p_1 and normal displacement u_3 on Γ_0 (see Eq. (3)). Consequently, the normal displacement field u_3 should be an odd function of x_1. Figures 8 show the graphs of $x_1 \mapsto u_3(x_1, x_3, t)$ with $x_3 = 0$ at $t = 1.56\,\mu$s (Fig. 8(A)), $t = 2.06\,\mu$s (Fig. 8(B)), $t = 2.94\,\mu$s (Fig. 8(C)), $t = 5.89\,\mu$s (Fig. 8(D)), $t = 9.72\,\mu$s (Fig. 8(E)), $t = 13.55\,\mu$s (Fig. 8(F)), $t = 15.31\,\mu$s (Fig. 8(G)), $t = 119.88\,\mu$s (Fig. 8(H)). For this particular example and for $x_3 = 0$, it should be noted that $x_1 \mapsto u_3(x_1, x_3, t)$ is an odd function which is coherent with the results presented in Figures 8 . Figures 9 show the graphs of $x_1 \mapsto u_1(x_1, x_3, t)$ with $x_3 = 0$ at $t = 1.56\,\mu$s (Fig. 9(A)), $t = 2.06\,\mu$s (Fig.

9(B)), $t = 2.94\,\mu$s (Fig. 9(C)), $t = 5.89\,\mu$s (Fig. 9(D)), $t = 9.72\,\mu$s (Fig. 9(E)), $t = 13.55\,\mu$s (Fig. 9(F)), $t = 15.31\,\mu$s (Fig. 9(G)), $t = 119.88\,\mu$s (Fig. 9(H)). For this particular example, it should be noted that tangential displacement field u_1 has no symmetry property on Γ_0.

9 CONCLUSION

We have presented a method dedicated to the simulation of the transient elastic wave propagation in multilayer unbounded media. The method is especially efficient to investigate the propagation of broadband pulses thanks to a time-domain formulation. To take advantage of the symmetry of the multilayer configuration, we have used a spectral formulation in the unbounded direction of the layers. The boundary problem is reduced to a 1D-space, time-domain, problem and solved with the finite element method using the implicit unconditionally stable Newmark scheme to solve the problem in time. The weak formulation associated to the 1D boundary value problem and the corresponding finite element approximation have been constructed for the purposes of this work. The efficiency of the method is illustrated in numerical example presented for a coupled elastodynamics and acoustic problem in a three-layer configuration.

Although the method is presented in a 2D-configuration, the formulation of its 3D counterpart based on the equations given in this paper is straightforward. The method is intrinsically restricted to academic geometrical configurations: systems of plane unbounded layers. Nevertheless it can be used to simulate complex situation such has propagation in arbitrarily anisotropic media; arbitrary heterogeneity in depth: arbitrary profile of the evolution of properties (elasticity or density) with depth in each layer; interaction with very fine layers, etc. Furthermore, the method can easily be extended to study transient wave propagation in viscoelastic media.

References

[1] J. D. Achenbach, *Wave Propagation in Elastic Solids.* (North-Holland/American Elsevier, 1987)

[2] K. Aki, P.G. Richard, *Quantitative Seismology: Theory and Methods.* (1980)

[3] A. Akyurtlu , D. H. Werner, "BI-FDTD: a novel finite-difference time-domain formulation for modeling wave propagation in bi-isotropic media", IEEE Trans. on Antennas Propagat., **52**(2), 416-425, (2004)

[4] K. J. Bathe, E. L. Wilson, *Numerical Methods in Finite Element Analysis*, (New York/Prentice-Hall, 1976)

[5] P. Bonnet and al., "Numerical modeling of scattering problems using a time domain finite volume method", J. Electromagn. Waves Appl.,1165-1189, (1997)

[6] E. Bossy and al., "Bidirectional axial transmission can improve accuracy and precision of ultrasonic velocity measurement in cortical bone: a validation on test materials", IEEE Trans Ultrason Ferroelectr Freq Control, **51**(1), 71-9 (2004)

[7] L.M. Brekhovskikh, *Waves in Layered Media. Applied Mathematics and mechanics.* (San Diego/Academic Press, 1973)

[8] L. Cagniard, *Reflection and Refraction of Progressive Seismic Waves.* 1962.

[9] D. Clouteau, M. Arnst, T.M. Al-Hussainia, G. Degrande, "Freefield vibrations due to dynamic loading on a tunnel embedded in a stratified medium", Journal of Sound and Vibration, **283**(1-2), 173-199 (2005)

[10] N.X. Dong, E.X. Guo, "The dependence of transversely isotropic elasticity of human femoral cortical bone on porosity", Journal of Biomechanics, **37**(8), 1281-1287 (2004)

[11] A.T. de Hoop, "A modification of Cagniard's method for solving seismic pulse problems", Applied Scientific Research, **8**, 349-356, (1960)

[12] A.T. de Hoop, "Acoustic radiation from an impulsive point source in a continuously layered fluid; an analysis based on the Cagniard method", J. Acoust. Soc. Am., **88**(5), 2376-2388, (1990)

[13] B. Faverjon, C. Soize, "Equivalent acoustic impedance model. Part 2: analytical approximation", Journal of Sound and Vibration, **276**(3-5), 593-613, (2004)

[14] M. W. Feise, J. B. Schneider, P. J. Bevelacqua, "Finite-difference and pseudospectral time-domain methods applied to backward-wave metamaterials", IEEE Trans. Antennas Propagat., **52**(11), 2955-2962, (2004)

[15] P. Fellinger, R. Marklein, K.J. Langenberg and al., "Numerical modeling of elastic-wave propagation and scattering with efit - elastodynamic finite integration technique", Wave Motion **21**(1): 47-66 (1995)

[16] O. P. Gandhi, B.-Q. Gao, and J.-Y. Chen, "A frequency-dependent finite difference time-domain formulation for general dispersive media", IEEE Trans. on Microwave Theory Tech., **41**, 658-664, (1993)

[17] D. Givoli, J.B. Keller, "A finite-element method for large domains", Computer Methods in Applied Mechanics and Engineering, **76**(1): 41-66, (1989)

[18] D. Givoli, "Nonreflecting boundary-conditions",Journal of Computational Physics, **94**(1): 1-29, (1991)

[19] D. Givoli, "Numerical methods for mechanics problems in infinite do-

mains", Studies in Applied Mechanics, 1992
[20] D. Givoli, "Recent advances in the DtN FE Method", Archives of Computational Methods in Engineering, **6**(2): 71-116, (1999)
[21] D. Givoli, B. Neta, I. Patlashenko, "Finite element analysis of time-dependent semi-infinite wave-guides with high-order boundary treatment", International Journal for Numerical Methods in Engineering, **58**(13): 1955-1983, (2003)
[22] K. F. Graff *Wave Motion in Elastic Solids*, (Oxford University Press, 1975)
[23] P. Joly, "Variational methods for time-dependant wave propagation problems", *Computational wave propagation, direct and inverse problems*, LNCSE, 201-264, 2003
[24] H.M. Jurgens, D.W. Zingg, "Numerical solution of the time-domain Maxwell equations using high-accuracy finite-difference methods", SIAM Journal on Scientific Computing, **22**(5): 1675-1696, (2001)
[25] J.H.M.T. van der Hijden, *Propagation of transient elastic waves in stratified anisotropic media*, 1987
[26] B.L.N. Kennett, *Seismic wave propagation in stratified media*. (1983)
[27] J. Kim, A. Papageorgiou, " Discrete wave-number boundary-element method for 3-D scattering problems ", Journal of Engineering Mechanics, **119**(3), 603-625 (1993)
[28] S.C. Kong, S.J. Lee, J.H. Lee, Y.W. Choi, "Numerical analysis of traveling-wave photodetectors' bandwidth using the finite-difference time-domain method", IEEE Transactions on Microwave Theory and Techniques, **50**(11), 2589-2597, (2002)
[29] S. W. Liu, S. K. Datta, T. H. Ju, "Transient scattering of Rayleigh-Lamb waves by a surface-breaking crack. Comparison of numerical simulation and experiment", Journal of Nondestructive Evaluation, **10**(3), 111-126 (1991)
[30] R. Luebbers, F.P. Hunsberger, K. Kunz, R. Standler, M. Schneider, "A frequency-dependent finite-difference time-domain formulation for dispersive materials", IEEE Trans. Electromagn. Compat., **32**, 222-227, (1990)
[31] K. Macocco, Q. Grimal, S. Naili, C. Soize, "Elastoacoustic model with uncertain mechanical properties for ultrasonic wave velocity prediction: Application to cortical bone evaluation", J. Acoust. Soc. Am., **119**(2), 729–740 (2006)
[32] N.K. Madsen, R.W. Ziolkowski,"Numerical-Solution of maxwell equations in the time domain using irregular nonorthogonal grids", Wave Motion, **10**(6): 583-596, (1988)
[33] A. Mourad, M. Deschamps, "Lamb's problem for an anisotropic half-space studied by the Cagniard-de Hoop method", J. Acoust. Soc. Am., **97**, 3194-3197 (1995)
[34] C. C. Ma, S. W. Liu, C. M. Chang, "Inverse calculation of material parameters for a thin-layer system using transient elastic waves", J. Acoust. Soc. Am., **112**(3), 811-821 (2002)
[35] R. Ohayon, C. Soize, *Structural Acoustics and Vibration, Academic Press*, New York, 1998
[36] S. Palaniswamy, W.F. Hall, V. Shankar, "Numerical solution to Maxwell's equations in the time domain on nonuniform grids", Radio Science, **31**(4), 905-912, (1996)

[37] A. D. Pierce, *Acoustics: An Introduction to its Physical Principles and Applications*, Acoust. Soc. Am. Publications on Acoustics, Woodbury, NY, U.S.A (originally published in 1981, McGrawHill, New York)
[38] E. Savin, D. Clouteau, "Elastic wave propagation in a 3-D unbounded random heterogeneous medium coupled with a bounded medium. Application to seismic soil-structure interaction (SSSI)", International Journal for numerical Methods in Engineering **54**(4), 607-630 (2002)
[39] X. Sheng, C. J. C. Jones, D. J. Thompson, "Prediction of ground vibration from trains using the wavenumber finite and boundary element methods", Journal of Sound and Vibration, **293**(3-5), 575-586, (2006)
[40] D. M. Sullivan, "Frequency-dependent FDTD methods using Z transforms", IEEE Trans. Antennas Propagat., **40**, 1223-1230, (1992)
[41] A. Taflove, "Review of the formulation and applications of the finite-difference time-domain method for numerical modeling of electromagnetic wave interactions with arbitrary structures", Wave Motion, **1**(6), 547-582, (1988)
[42] A. Taflove, *Computational Electrodynamics: The Finite Difference Time Domain Method*, Norwood, MA: Artech House, 1995.
[43] P. Thoma, T. Weiland, "Numerical stability of finite difference time domain methods", IEEE Transactions on Magnetics, **34**(5), 2740-2743, (1998)
[44] M.D. Verweij, "Modeling space-time domain acoustic wave fields in media with attenuation: The symbolic manipulation approach", J. Acoust. Soc. Am.,**97**(2), 831-843 (1995)
[45] J. Virieux, "P-SV wave propagation in heterogenous media: Velocity-stress finite-difference method", Geophysics, **51**(4), 889-901 (1986)
[46] C. Zhou, N. N. Hsu, J. S. Popovics, J. D. Achenbach, "Response of two layers overlaying a half-space to a suddenly applied point force", Wave Motion, **31**, 255-272 (2000)
[47] O. C. Zienkiewicz, R. L. Taylor *The finite element method*, McGraw-Hill, (1991)

A Sesquilinear forms and antilinear form for the weak formulation

The weak formulation presented in section 5 introduces, respectively, the positive-definite and definite sesquilinear forms a_1 and b_1 defined on $\mathscr{C}_1 \times \mathscr{C}_1$, the sesquilinear form r_1 defined on $\mathscr{C} \times \mathscr{C}_1$, the antilinear form f_1 defined on $\mathscr{C}_1$, the sesquilinear forms positive-definite and positive a_2 and b_2 defined on $\mathscr{C}_2 \times \mathscr{C}_2$, the sesquilinear form r_2 defined on $\mathscr{C} \times \mathscr{C}_2$, the positive-definite sesquilinear form a defined on $\mathscr{C} \times \mathscr{C}$ and finally, the sesquilinear form b defined on $\mathscr{C} \times \mathscr{C}$ which are such that

$$a_1(\widehat{p}_1, \delta p_1) = \frac{1}{K_1} \int_0^{z_1} \widehat{p}_1 \, \overline{\delta p_1} \, dx_3 \tag{42}$$

$$b_1(\widehat{p}_1, \delta p_1) = \frac{1}{\rho_1} \int_0^{z_1} \frac{\partial \widehat{p}_1}{\partial x_3} \overline{\frac{\partial \delta p_1}{\partial x_3}}\, dx_3 \tag{43}$$

$$r_1(\widehat{\mathbf{u}}, \delta p_1) = \widehat{u}_3(0)\overline{\delta p_1(0)} \tag{44}$$

$$f(\delta p_1; t) = F(t)\, e^{ik_1 x_1^S}\, \overline{\delta p_1(x_3^S)} \tag{45}$$

$$m(\widehat{\mathbf{u}}, \delta \mathbf{u}) = \int_z^0 \rho \langle \widehat{\mathbf{u}}, \overline{\delta \mathbf{u}} \rangle dx_3 \tag{46}$$

$$s_1(\widehat{\mathbf{u}}, \delta \mathbf{u}) = \int_z^0 \langle [D_1] \frac{\partial \widehat{\mathbf{u}}}{\partial x_3}, \overline{\frac{\partial \delta \mathbf{u}}{\partial x_3}} \rangle dx_3 \tag{47}$$

$$s_2(\widehat{\mathbf{u}}, \delta \mathbf{u}) = \int_z^0 \langle [D_2]\, \widehat{\mathbf{u}}, \overline{\delta \mathbf{u}} \rangle dx_3 \tag{48}$$

$$s_3(\widehat{\mathbf{u}}, \delta \mathbf{u}) = \int_z^0 \left(\langle [D_3]\, \widehat{\mathbf{u}}, \overline{\frac{\partial \delta \mathbf{u}}{\partial x_3}} \rangle - \langle [D_3]\, \overline{\delta \mathbf{u}}, \frac{\partial \widehat{\mathbf{u}}}{\partial x_3} \rangle \right) dx_3 \tag{49}$$

$$a_2(\widehat{p}_2, \delta p_2) = \frac{1}{K_2} \int_{z_2}^z \widehat{p}_2\, \overline{\delta p_2}\, dx_3 \tag{50}$$

$$b_2(\widehat{p}_2, \delta p_2) = \frac{1}{\rho_2} \int_{z_2}^z \frac{\partial \widehat{p}_2}{\partial x_3} \overline{\frac{\partial \delta p_2}{\partial x_3}}\, dx_3 \tag{51}$$

$$r_2(\widehat{\mathbf{u}}, \delta p_2) = \widehat{u}_3(z)\overline{\delta p_2(z)} \tag{52}$$

in which $\langle \cdot, \cdot \rangle$ means the usual euclidean inner product on $\mathbb{R}^2$ and where

$$[D_1] = \begin{bmatrix} \widetilde{c}_{33}/2 & \widetilde{c}_{32}/\sqrt{2} \\ \widetilde{c}_{23}/\sqrt{2} & \widetilde{c}_{22} \end{bmatrix}, [D_2] = \begin{bmatrix} \widetilde{c}_{11} & \widetilde{c}_{13}/\sqrt{2} \\ \widetilde{c}_{31}/\sqrt{2} & \widetilde{c}_{33}/2 \end{bmatrix}, [D_3] = \begin{bmatrix} \widetilde{c}_{31}/\sqrt{2} & \widetilde{c}_{33}/2 \\ \widetilde{c}_{21} & \widetilde{c}_{23}/\sqrt{2} \end{bmatrix}.$$

It is assumed that $[D_2]$ is an invertible matrix.

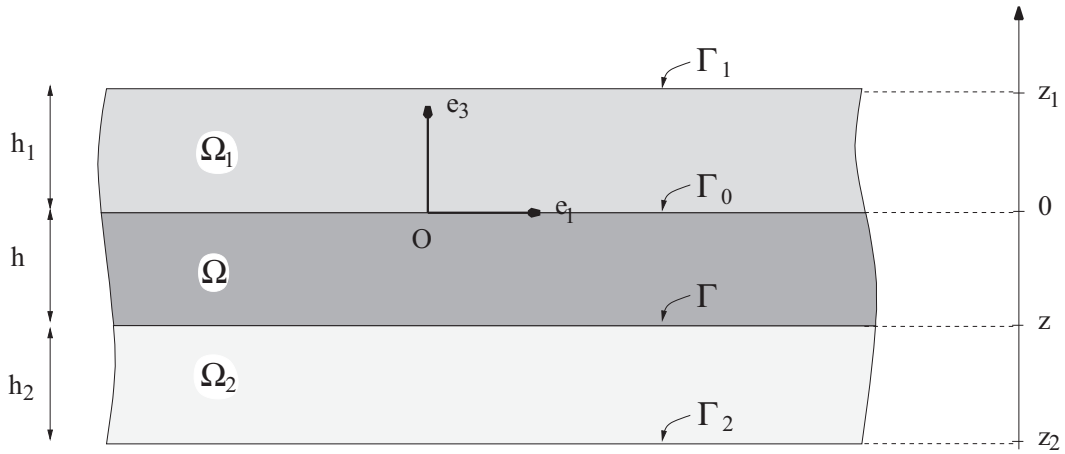

Fig 1. Geometric configuration

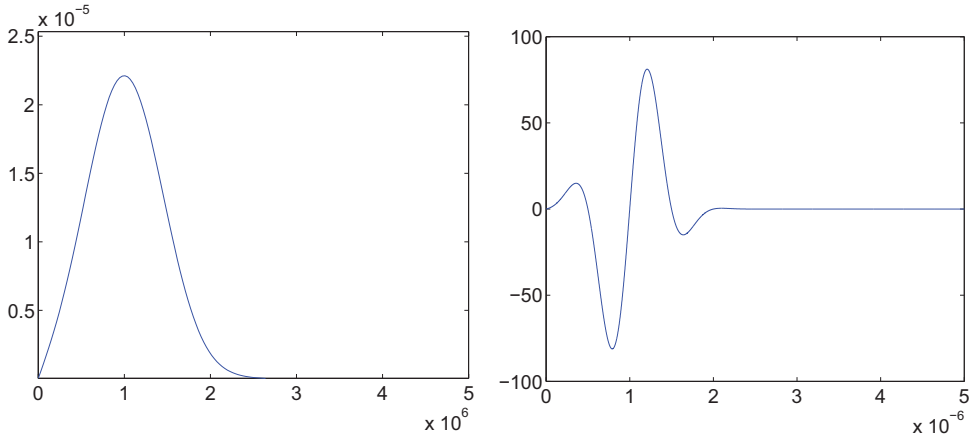

Fig 2. Definition of the function F. Graphs of the power spectrum of F (left) and function $t \mapsto F(t)$ (right). Vertical axis: power spectrum (left) and F(t) (right). Horizontal axis: frequency in Hz (left) and t in s (right).

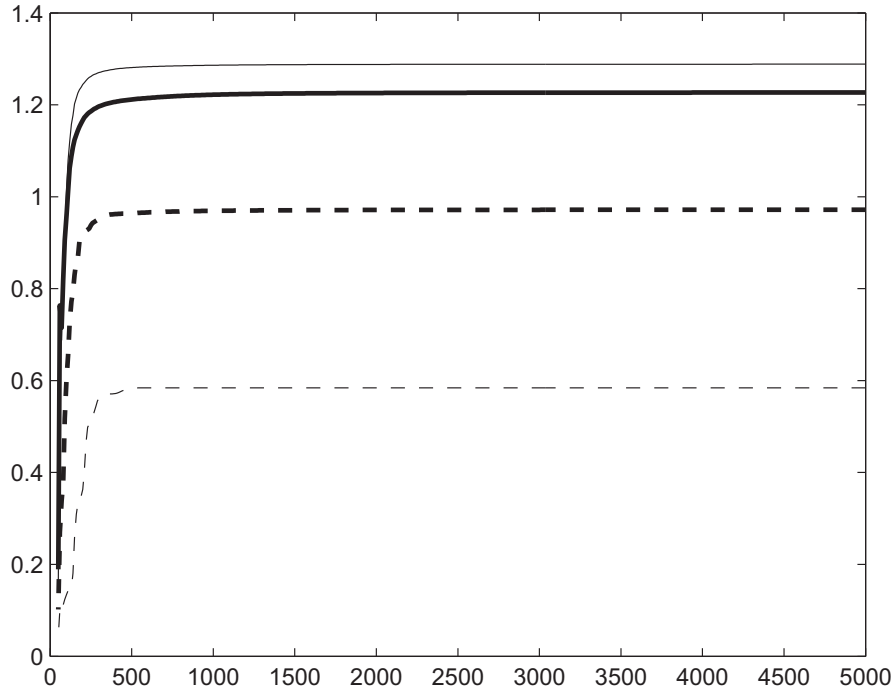

Fig 3. Convergence analysis with respect to N. Graphs of the function $N \mapsto \mathrm{conv}(N, M; x_1, x_3)$ *with* $M = 8192$ *and* $x_3 = 2 \times 10^{-3}$ *m and for* $x_1 = 8 \times 10^{-3}$ *m (thick solid line),* $x_1 = 12 \times 10^{-3}$ *m (thin solid line),* $x_1 = 20 \times 10^{-3}$ *m (thick dashed line) and* $x_1 = 28 \times 10^{-3}$ *m (thin dashed line). Vertical axis:* $\mathrm{conv}(N, M; x_1, x_3)$. *Horizontal axis: N*

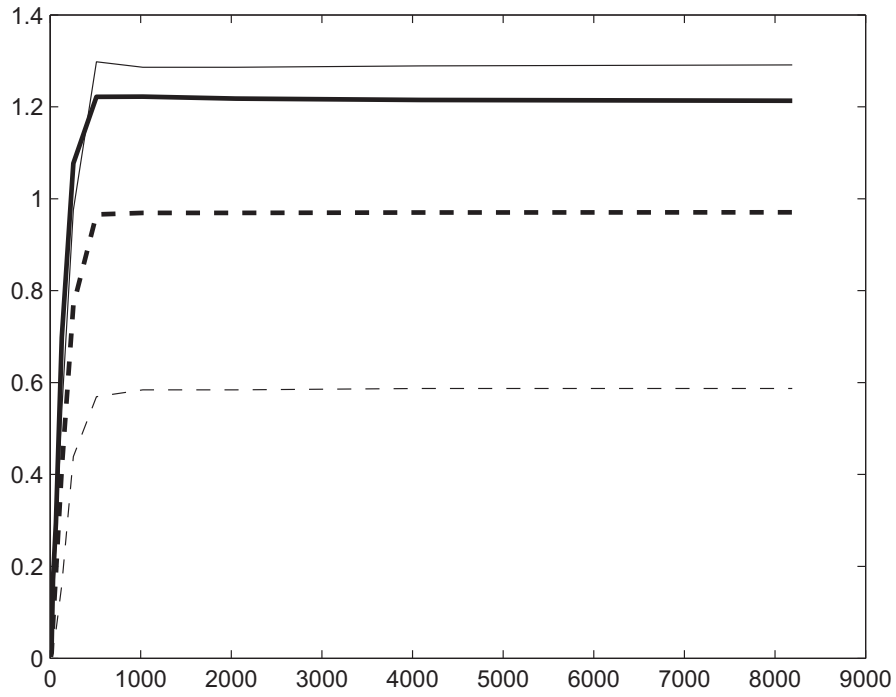

Fig 4. Convergence analysis with respect to M. Graphs of the function $M \mapsto \mathrm{conv}(N, M; x_1, x_3)$ *with* $N = 5000$ *and* $x_3 = 2{\times}10^{-3}$ *m and for* $x_1 = 8{\times}10^{-3}$ *m (thick solid line),* $x_1 = 12 \times 10^{-3}$ *m (thin solid line),* $x_1 = 20 \times 10^{-3}$ *m (thick dashed line) and* $x_1 = 28 \times 10^{-3}$ *m (thin dashed line). Vertical axis:* $\mathrm{conv}(N, M; x_1, x_3)$. *Horizontal axis: M*

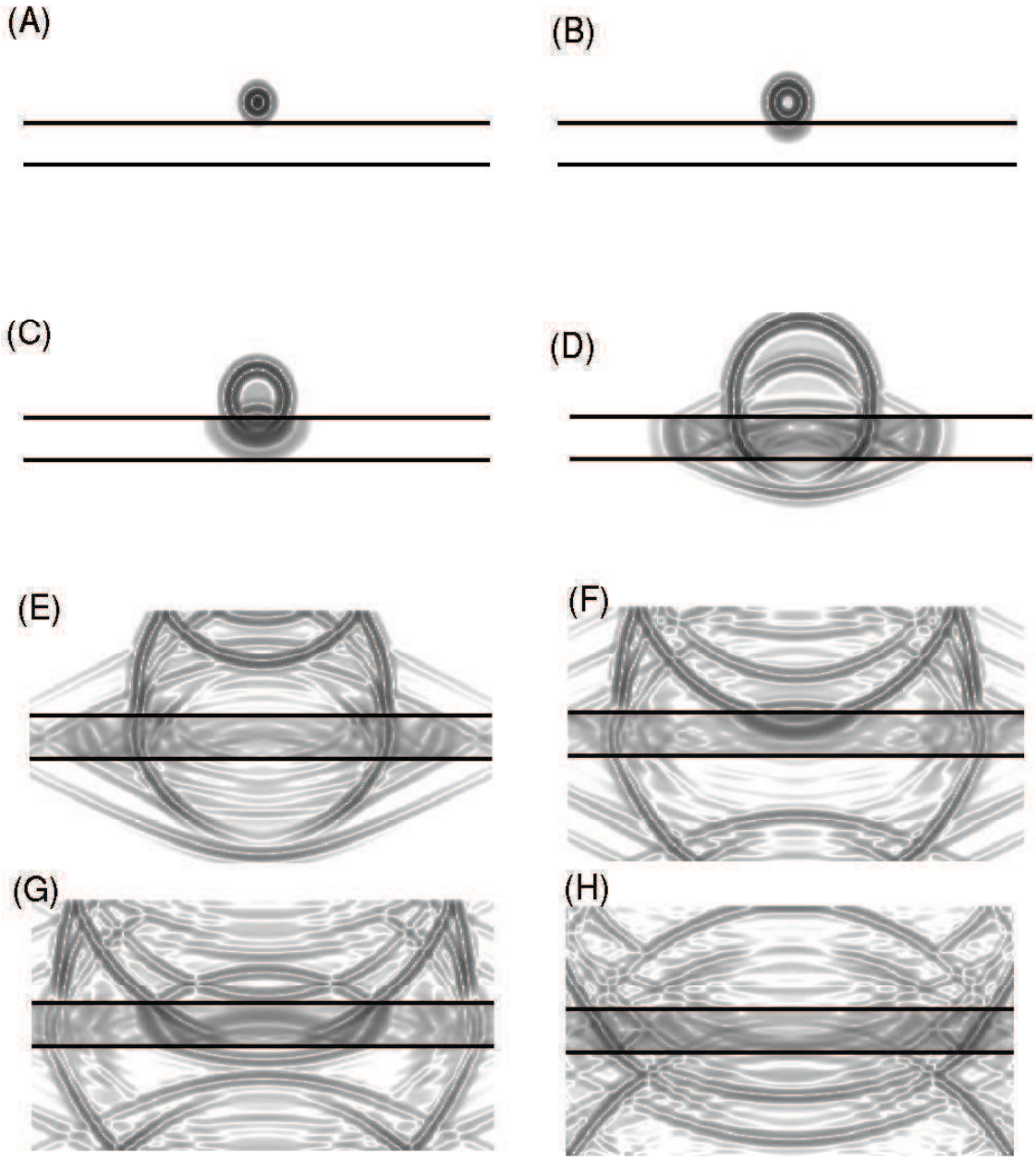

Fig 5. Wave propagation in the three layers (pressure field in the fluid layers and von Mises stress field in the elastic layer) at $t = 1.56\,\mu$s *(Fig. A),* $t = 2.06\,\mu$s *(Fig. B),* $t = 2.94\,\mu$s *(Fig. C),* $t = 5.89\,\mu$s *(Fig. D),* $t = 9.72\,\mu$s *(Fig. E),* $t = 13.55\,\mu$s *(Fig. F),* $t = 15.31\,\mu$s *(Fig. G),* $t = 119.88\,\mu$s *(Fig. H).*

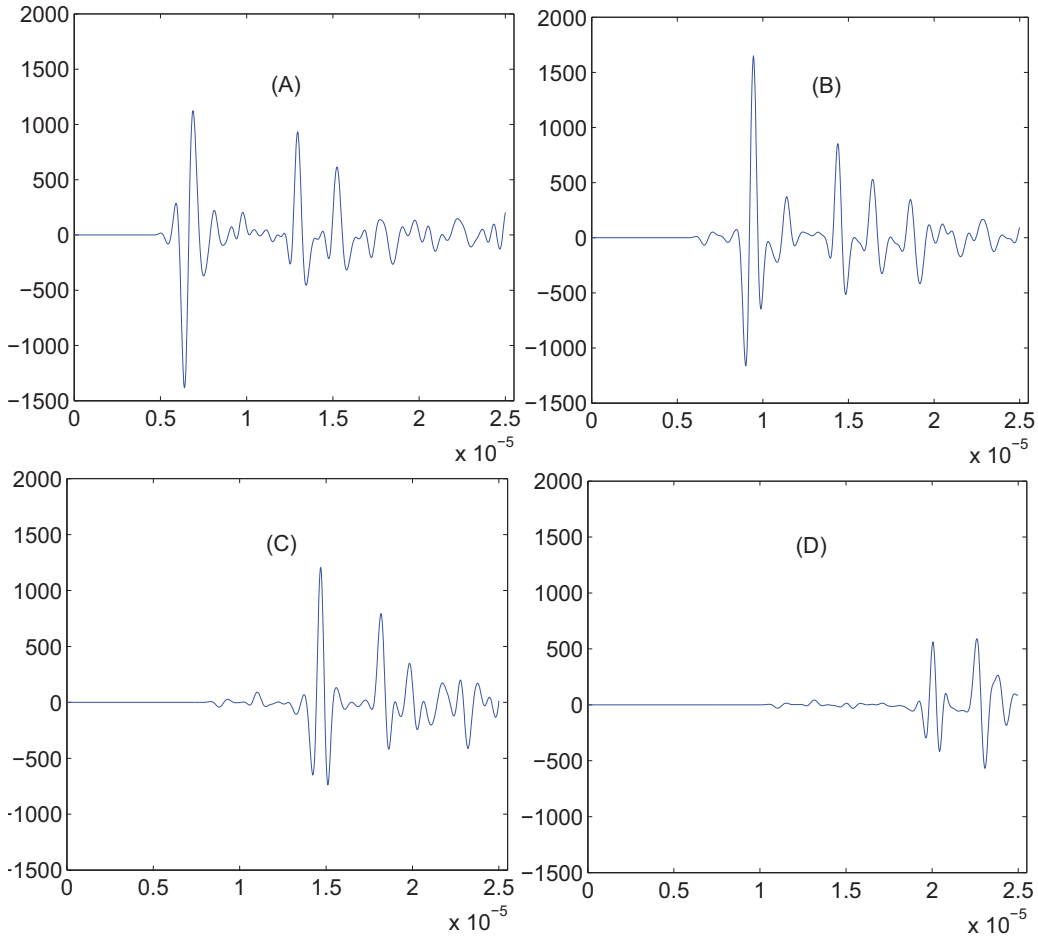

Fig 6. Evolution of the pressure disturbance in the fluid occupying Ω_1. *Graphs of function* $t \mapsto p_1(x_1, x_3, t)$ *with* $x_3 = 2 \times 10^{-3}$ *m and for* $x_1 = 8 \times 10^{-3}$ *m (fig. A),* $x_1 = 12 \times 10^{-3}$ *m (fig. B),* $x_1 = 20 \times 10^{-3}$ *m (fig. C) and* $x_1 = 28 \times 10^{-3}$ *m (fig. D). Vertical axis:* $\mathrm{conv}(N, M; x_1, x_3)$. *Horizontal axis:* t. *Vertical axis :* $p_1(x_1, x_3, t)$

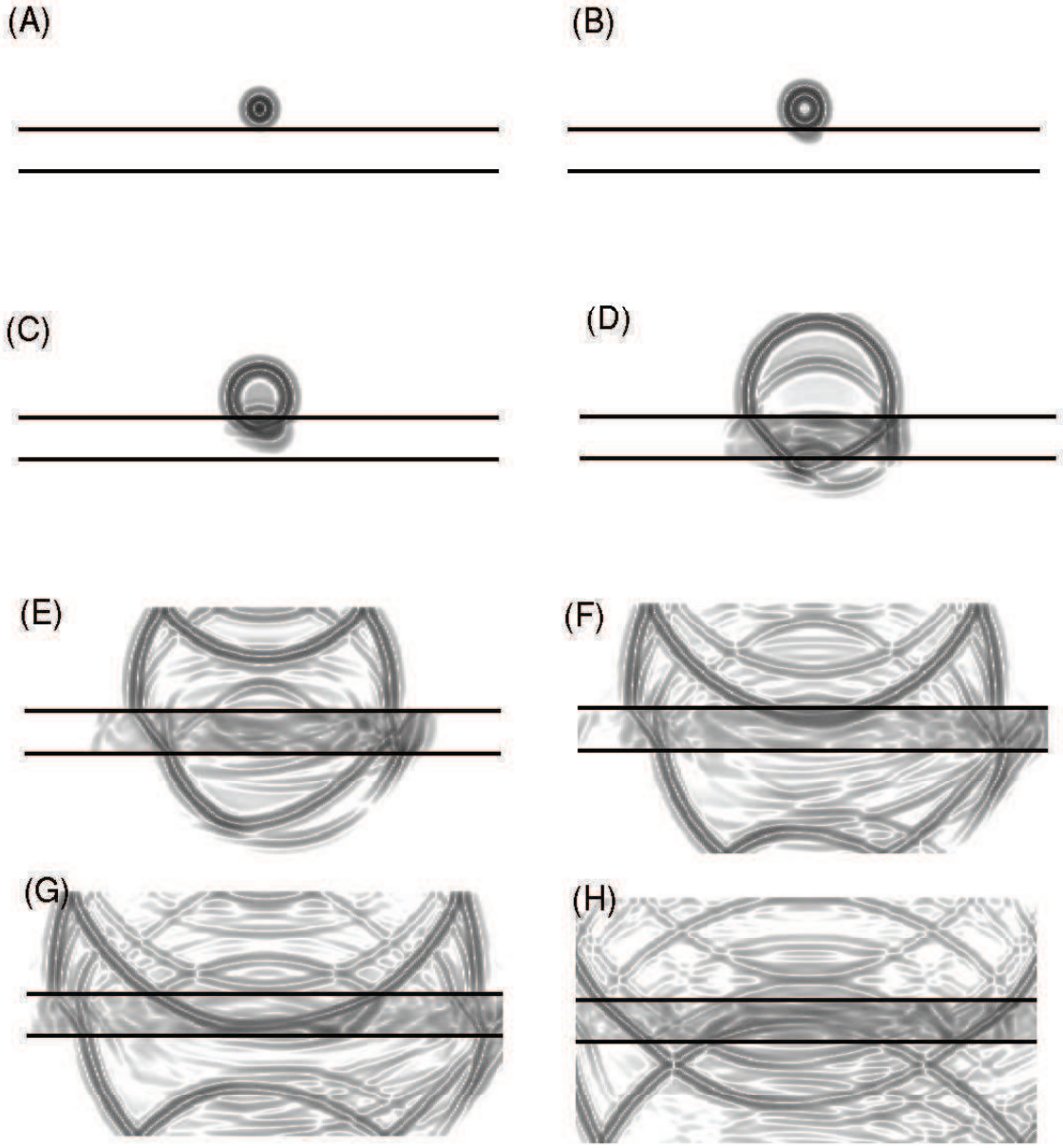

Fig 7. Wave propagation in the three layers (pressure field in the fluid layers and von Mises stress field in the elastic layer) at $t = 1.56\,\mu$s *(Fig. A),* $t = 2.06\,\mu$s *(Fig. B),* $t = 2.94\,\mu$s *(Fig. C),* $t = 5.89\,\mu$s *(Fig. D),* $t = 9.72\,\mu$s *(Fig. E),* $t = 13.55\,\mu$s *(Fig. F),* $t = 15.31\,\mu$s *(Fig. G),* $t = 119.88\,\mu$s *(Fig. H).*

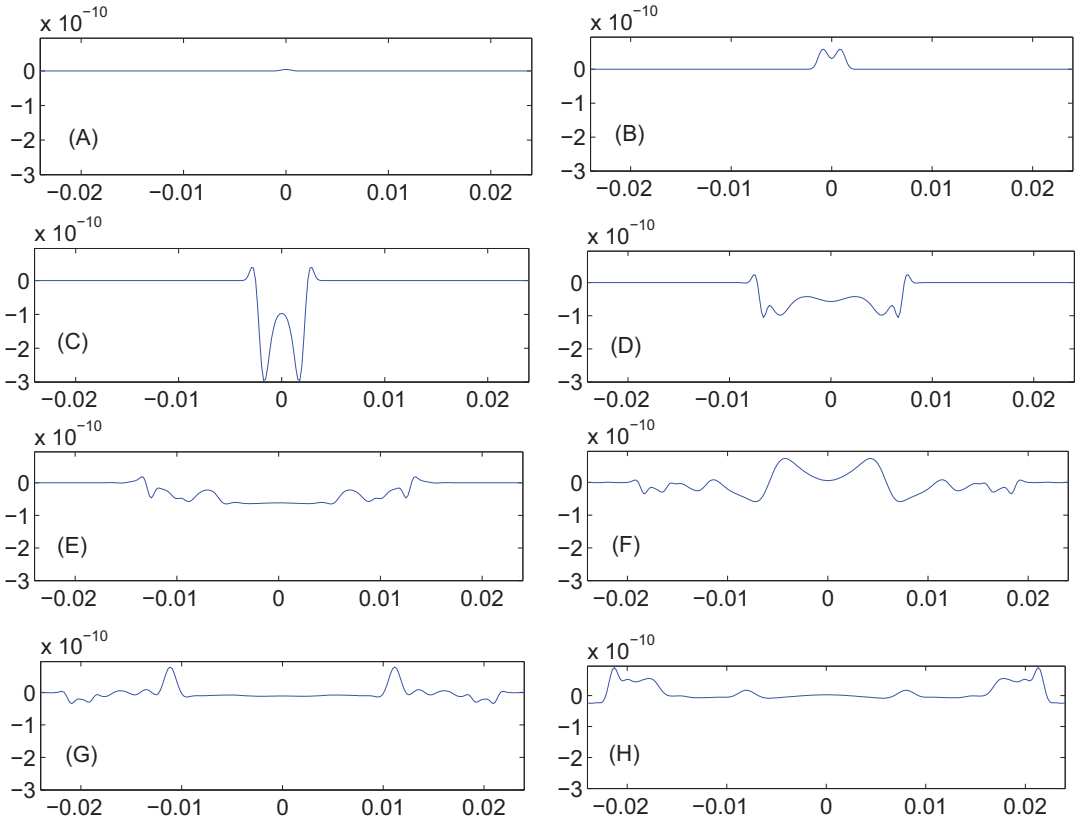

Fig 8. Normal displacement field of the solid layer on the interface Γ_0 *at* $t = 1.56\,\mu$s *(Fig. A),* $t = 2.06\,\mu$s *(Fig. B),* $t = 2.94\,\mu$s *(Fig. C),* $t = 5.89\,\mu$s *(Fig. D),* $t = 9.72\,\mu$s *(Fig. E),* $t = 13.55\,\mu$s *(Fig. F),* $t = 15.31\,\mu$s *(Fig. G),* $t = 119.88\,\mu$s *(Fig. H). Horizontal axis :* x_1 *(m). Vertical axis :* $u_3(x_1, x_3)$ *with* $x_3 = 0$.

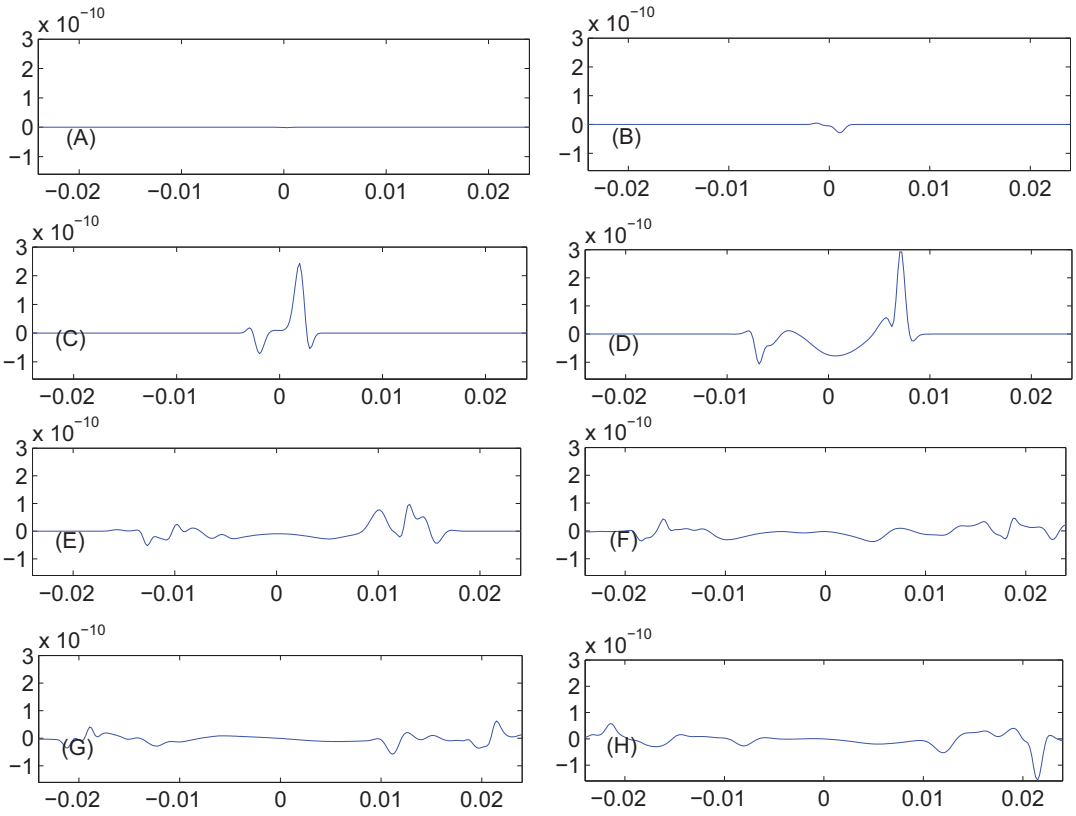

Fig 9. Tangential displacement field of the solid layer on the interface Γ_0 *at* $t = 1.56\,\mu$s *(Fig. A),* $t = 2.06\,\mu$s *(Fig. B),* $t = 2.94\,\mu$s *(Fig. C),* $t = 5.89\,\mu$s *(Fig. D),* $t = 9.72\,\mu$s *(Fig. E),* $t = 13.55\,\mu$s *(Fig. F),* $t = 15.31\,\mu$s *(Fig. G),* $t = 119.88\,\mu$s *(Fig. H). Horizontal axis :* x_1 *(m). Vertical axis :* $u_1(x_1, x_3)$ *with* $x_3 = 0$.